CONTINUAL HYPERBOLIC LEARNING OF INSTANCES AND CLASSES

Melika Ayoughi
University of Amsterdam,
m.ayoughi@uva.nl

Mina GhadimiAtigh*
University of Amsterdam,
m.ghadimiatigh@uva.nl

Mohammad Mahdi Derakhshani*
University of Amsterdam,
m.m.derakhshani@uva.nl

Cees Snoek
University of Amsterdam,
c.g.m.snoek@uva.nl

Pascal Mettes
University of Amsterdam,
p.s.m.mettes@uva.nl

Paul Groth
University of Amsterdam,
p.t.groth@uva.nl

arXiv:2506.10710v1 [cs.CV] 12 Jun 2025

ABSTRACT

Continual learning has traditionally focused on classifying either instances or classes, but real-world applications, such as robotics and self-driving cars, require models to handle both simultaneously. To mirror real-life scenarios, we introduce the task of continual learning of instances *and* classes, at the same time. This task challenges models to adapt to multiple levels of granularity over time, which requires balancing fine-grained instance recognition with coarse-grained class generalization. In this paper, we identify that classes and instances naturally form a hierarchical structure. To model these hierarchical relationships, we propose HyperCLIC, a continual learning algorithm that leverages hyperbolic space, which is uniquely suited for hierarchical data due to its ability to represent tree-like structures with low distortion and compact embeddings. Our framework incorporates hyperbolic classification and distillation objectives, enabling the continual embedding of hierarchical relations. To evaluate performance across multiple granularities, we introduce continual hierarchical metrics. We validate our approach on EgoObjects, the only dataset that captures the complexity of hierarchical object recognition in dynamic real-world environments. Empirical results show that HyperCLIC operates effectively at multiple granularities with improved hierarchical generalization.

1 INTRODUCTION

Continual learning addresses a long-standing challenge in machine learning: learning from new classes often leads to catastrophic forgetting of old classes (Kirkpatrick et al., 2017; Wu et al., 2019; Magistri et al., 2024; Lyle et al., 2024; De Lange et al., 2021; Wang et al., 2024). To mitigate this, numerous solutions have been proposed, including data replay (Bang et al., 2021; Wang et al., 2021), regularization (Yin et al., 2021; Lee et al., 2020), and knowledge distillation (Kang et al., 2022; Dong et al., 2022). While these methods primarily focus on class-level discrimination, fewer works have expanded the scope to instance-level continual learning. In robotics, for example, classifying specific instances of objects enables robots to make informed decisions about their use or placement (Ammirato, 2019; Singh et al., 2014; Held et al., 2016). Several benchmarks have been developed to recognize instances under varying conditions such as illumination, occlusion, or background (Borji et al., 2016; Lomanco & Maltoni, 2017; She et al., 2020). Parshotam & Kilickaya (2020) and Kilickaya & Vanschoren (2023) address incremental instance recognition using metric learning under an object re-identification setting and self-supervised learning respectively. The recent EgoObjects (Zhu et al., 2023) benchmark and its instance-level continual challenge (Pellegrini et al., 2022) further highlight the complexity, scale and open-ended nature of instance-level recognition in dynamic real-world environments.

In real-life scenarios, recognition at a *single* granularity level is often insufficient. For critical domains such as robotics, self-driving cars, and medical imaging, it is crucial that even if instance-level predictions are incorrect, class-level predictions remain accurate to prevent catastrophic outcomes and enable quick generalization to new instances. This is challenging because class-level continual learning, by design, is invariant to specific instances, while instance-level

* Equal contribution.

continual learning without class-level awareness risks significant errors. We introduce the problem of *joint* instance- and class-level continual learning, which aims to perform recognition simultaneously at both levels of granularity.

To tackle this challenge, we leverage the inherent hierarchical structure of instances and classes. Classes form a coarse-to-fine hierarchy (Fellbaum, 2010; Deng et al., 2009), and instances add an additional layer to this hierarchy (Yan et al., 2024). Figure 1 illustrates this hierarchical organization. Theoretically, hyperbolic space is known for its ability to embed tree-structured data with minimal distortion (Sarkar, 2011). This property stems from two fundamental characteristics of hyperbolic geometry: negative curvature and exponential volume growth. In contrast to Euclidean space, where polynomial volume growth leads to inevitable distortion when embedding branching in high dimensions, hyperbolic space naturally accommodates hierarchical representations. This geometric advantage precisely matches the exponential properties in real-world taxonomies. Thus, hyperbolic learning has been used in many hierarchical computer vision tasks (Ibrahimi et al., 2024a; Desai et al., 2023; Mettes et al., 2024; Ge et al., 2023; Hong et al., 2023). Due to the strong hierarchical nature of the problem of joint class- and instance-level continual learning, hyperbolic learning provides a natural solution for preserving such relationships during incremental learning. We propose HyperCLIC, a hyperbolic continual learner that embeds this hierarchy in hyperbolic space for *joint* instance- and class-level recognition. Our contributions are threefold: (i) we formally define the task of continual learning of instances and classes and introduce continual hierarchical metrics to measure accuracy at both levels and evaluate the severity of hierarchical mistakes; (ii) we introduce HyperCLIC, which employs hyperbolic classification and distillation losses to enable incremental learning while preserving hierarchical relationships; and (iii) we demonstrate the effectiveness of our approach on the EgoObjects benchmark, achieving strong performance across multiple granularities and making hierarchically better mistakes.

2 Literature Review

Continual Learning Continual learning is primarily studied under three main scenarios (Van de Ven et al., 2022; Chen & Liu, 2018): task-incremental, class-incremental, and domain-incremental learning. In task-incremental learning (Van de Ven et al., 2022; Kirkpatrick et al., 2017; Li & Hoiem, 2017), a model is trained on incremental tasks with clear boundaries. The task ID is known during test time. In contrast, in the class-incremental learning (Guo et al., 2022a; Kim et al., 2022; 2023; Wu et al., 2019; Rebuffi et al., 2017), the task ID is not provided ~~, making task-incremental a particular case of class-incremental~~. Domain-incremental (Shi & Wang, 2024; Garg et al., 2022b; Kalb et al., 2021; Mirza et al., 2022; Wang et al., 2022c) focuses on scenarios where the data distribution's incremental shift is explicitly modeled. Here, we focus on class-incremental learning. Regardless of continual scenarios, the main challenge of continual learning is to alleviate catastrophic forgetting with only limited access to the previous data (Evron et al., 2022; Shi et al., 2021). Catastrophic forgetting means that performance on previously learned tasks degrades significantly when learning new tasks. To address this, various strategies have been developed. Zhou et al. (2023) groups class-incremental methods into data-centric, model-centric, and algorithm-centric. Data-centric methods concentrate on solving class-incremental learning with exemplars by using data replay (Prabhu et al., 2020; Bang et al., 2021; Chaudhry et al., 2018a; Aljundi et al., 2019; Rolnick et al., 2019; Shin et al., 2017; Wang et al., 2021) or data regularization techniques (Lopez-Paz & Ranzato, 2017; Chaudhry et al., 2018b; Zeng et al., 2019). Model-centric methods either regularize the model parameters from drifting away (Kirkpatrick et al., 2017; Zenke et al., 2017; Yin et al., 2021; Lee et al., 2020) or dynamically expand the network structure for stronger representation ability (Yan et al., 2021; Zhou et al., 2022b; Wang et al., 2022a; Douillard et al., 2022). Algorithm-centric methods either utilize knowledge distillation (Hinton et al., 2015) to resist forgetting (Rebuffi et al., 2017; Kang et al., 2022; Li & Hoiem, 2017; Hou et al., 2019; Buzzega et al., 2020; Dong et al., 2022; Douillard et al., 2020) or rectify the bias in the model (Wu et al., 2019; Belouadah & Popescu, 2019; Zhou et al., 2022a; Zhao et al., 2020). Several recent works, such as Lee et al. (2023); Wang et al. (2022b); Muralidhara et al. (2024); Tran et al. (2024) highlight the importance of hierarchies in continual learning by exploring hierarchical task ordering configurations, our approach differs fundamentally: we treat hierarchy as prior knowledge for geometric representation learning rather than as a task configuration mechanism. These methods focus on ordering the tasks to first learn coarse-grained classes, with data labels continually expanding to more fine-grained

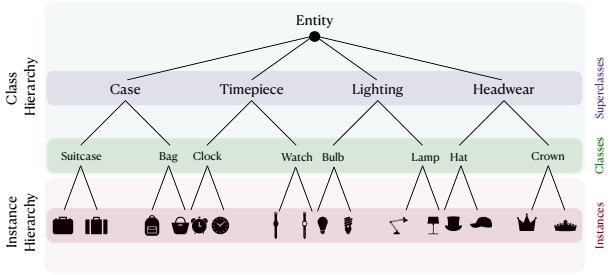


Figure 1: **Recognizing instances and classes simultaneously** is important in many real-world applications. By adding instances as an additional layer to the object hierarchy and learning representations that capture the joint hierarchy, we can classify samples at multiple levels of granularity.

classes. This distinction positions our work as complementary to - rather than competitive with - methods that modify the task sequence.

Hyperbolic Learning Hyperbolic learning has gained considerable attention in deep learning in embedding taxonomies and tree-like structures (Nickel & Kiela, 2017; Ganea et al., 2018a; Law et al., 2019; Nickel & Kiela, 2018), graphs (Liu et al., 2019; Chami et al., 2019; Bachmann et al., 2020; Dai et al., 2021), and text (Tifrea et al., 2018; Zhu et al., 2020; Dhingra et al., 2018; Leimeister & Wilson, 2018). Hyperbolic space is a space with constant negative curvature that can be thought of as a continuous version of a tree, making it a good choice to embed any finite tree while preserving the distances (Ungar, 2008; Hamann, 2018). Based on the tree-like behavior, Nickel & Kiela (2017) introduce a new approach to embed symbolic data in the Poincaré ball model, a particular hyperbolic space model. Ganea et al. (2018a) take a step forward and improve the Poincaré embeddings (Nickel & Kiela, 2017) using a model based on the geodesically convex entailment cones, showing the effectiveness when embedding data with a hierarchical structure. Furthermore, hyperbolic space has also been used to develop intermediate layers (Ganea et al., 2018a; Cho et al., 2019), and deep neural networks (Ganea et al., 2018b; Shimizu et al., 2020).

Following the initial success, hyperbolic space has shown success and gained attention in computer vision tasks in supervised and unsupervised learning (Mettes et al., 2024). Hyperbolic embeddings have shown benefits in classification and few-shot learning (Khrulkov et al., 2020; Gao et al., 2021; Guo et al., 2022b; Ghadimi Atigh et al., 2021), zero-shot learning (Liu et al., 2020; Hong et al., 2023), segmentation (Atigh et al., 2022; Chen et al., 2023), out-of-distribution generalization (Ganea et al., 2018b; van Spengler et al., 2023), uncertainty quantification (Atigh et al., 2022; Chen et al., 2023), contrastive learning (Yue et al., 2023; Ge et al., 2023), hierarchical representation learning (Long et al., 2020; Dhall et al., 2020; Doorenbos et al., 2024), generative learning (Cho et al., 2024; Dai et al., 2020; Mathieu & Nickel, 2020), and vision-language representation learning (Ibrahimi et al., 2024b; Desai et al., 2023). To our knowledge, Gao et al. (2023) is the only study that utilizes non-Euclidean geometries for class-level continual learning. Their approach introduces an expanding geometry of mixed-curvature space, targeting low-memory scenarios. We propose hyperbolic continual learning tailored for joint learning of instances and classes in a default memory regime.

3 Continual Learning of Instances and Classes

Task definition We follow a class-incremental learning setup, where new instance classes are introduced at each new task. Consider a sequence of T training tasks $\mathcal{D}^1, \mathcal{D}^2, ..., \mathcal{D}^T$ with non-overlapping instances, where $\mathcal{D}^t = (x_i^t, y_i^t)_{i=1}^{n_t}$ is the t-th incremental step with n_t training samples. Each $x_i^t \in \mathbb{R}^{\mathcal{D}}$ is an example of instance $y_i \in Y_t$, where Y_t is the label space of task t. We formalize the hierarchy of instances, classes, superclasses, and other nodes as a tree $\mathcal{T} = (V, E)$. Each label in Y_t corresponds to a leaf node label of tree $\mathcal{T}$, as detailed in tree definition. We only have access to samples of instances in $\mathcal{D}^t$ when training task t.

Tree definition The joint class-instance hierarchy $\mathcal{T} = (V, E)$ (Figure 1) consists of four types of vertices $V = V_I \cup V_C \cup V_S \cup V_O$ and four types of directed edges $E = E_{IC} \cup E_{CS} \cup E_{SO} \cup E_{OO}$. Vertices $V_I = \{i_1, i_2, ..., i_{n_I}\}$ are the set of instances, $V_C = \{c_1, c_2, ..., c_{nC}\}$ the set of classes that are parents of instances, $V_S = \{s_1, s_2, ..., s_{nS}\}$ the set of superclasses that are parents of classes, and $V_O = \{o_1, o_2, ..., o_{nO}\}$ are the set of other remaining nodes. Each node $v \in V$ corresponds to a distinct label. The number of nodes $|V|$ equals the number of all labels $|C|$ in the hierarchy. $E_{IC} = \{(i_j, c_k) \mid i_j \in V_I, c_k \in V_C\}$ represent edges between instances and classes, $E_{CS} = \{(c_k, s_m) \mid c_k \in V_C, s_m \in V_S\}$ edges between classes and superclasses, $E_{SO} = \{(s_m, o_p) \mid s_m \in V_S, o_p \in V_O\}$ edges between superclasses and other nodes, and $E_{OO} = \{(o_p, o_q) \mid o_p \in V_O, o_q \in V_O\}$ represents the remaining 1-hop hypernymy relations. In other words, E_{oo} represents all other remaining edges of the tree between nodes A and B, where neither A or B are instance (V_I), class (V_C), or superclass (V_S) nodes. This formalization defines the hierarchical relationships in a tree structure where each node V (instance, class, superclass, and other) except the root has one parent. Each instance V_I is a leaf node in the tree structure $\mathcal{T}$.

Continual hierarchical evaluation Evaluation is done using both standard and continual hierarchical metrics. The standard metrics include average forgetting, average accuracy, and per-task accuracies. In our work, the accuracy metric reflects the instance-level accuracy, so we refer to it as the continual instance-level accuracy. The instance-level accuracy on task t after incremental learning of task t' is defined as $\texttt{Acc}_{instance}^{tt'} = \frac{1}{n_t} \sum_{i=1}^{n_t} 1\{\hat{y_i}^{tt'} = y_i^t\}$, where $\hat{y_i}^{tt'}$ is the predicted class for instance label y_i^t evaluated on the test set of t-th task after incremental learning of the t'-th task. To evaluate continual hierarchical consistency and robustness, we report continual class-level and superclass-level accuracies, inspired by sibling and cousin accuracy in Ghadimi Atigh et al. (2021). For each sample x_i^t and its ground-truth instance label $y_i^t \in V_I$, let $p(y_i^t)$ be the parent class y_i^t and $gp(y_i^t)$ be the grandparent class of y_i^t. In class-level accuracy, a prediction is also correct if it shares a parent with the target class. The class-level accuracy on task

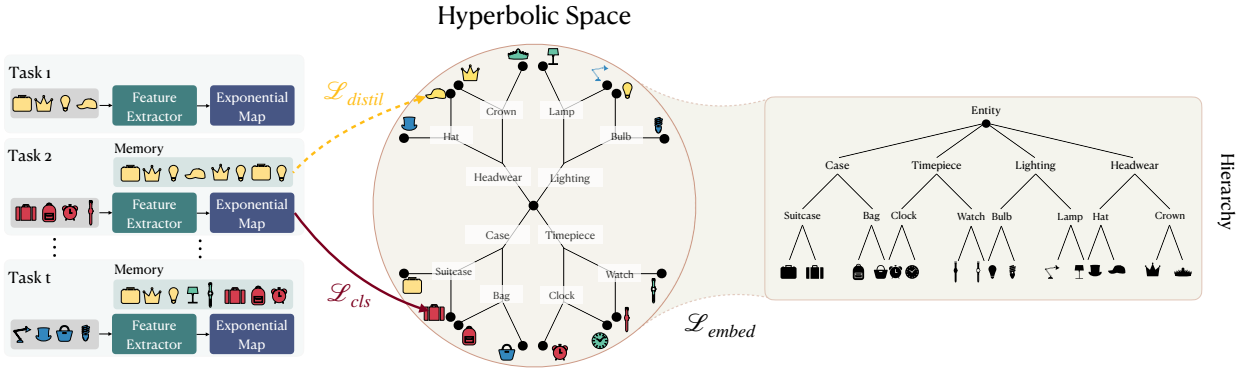


Figure 2: **Overview of HyperCLIC .** The class-instance hierarchy is projected into a shared hyperbolic space. When learning an instance, its samples go through the feature extractor and are mapped into the shared hyperbolic space using the exponential map. These samples are then pushed toward their hyperbolic instance prototype via classification loss and are encouraged to maintain hyperbolic logits from previous classes through hyperbolic distillation.

t after incremental learning of task t' is defined as $\texttt{Acc}^{tt'}_{class} = \frac{1}{n_t}\sum_{i=1}^{n_t} 1\{p(\hat{y_i}^{tt'}) = p(y_i^t)\}$. In the superclass-level accuracy, the predicted labels must share a grandparent with the target class to count as correct. The superclass-level accuracy on task t after incremental learning of task t' is defined as $\texttt{Acc}^{tt'}_{superclass} = \frac{1}{n_t}\sum_{i=1}^{n_t} 1\{gp(\hat{y_i}^{tt'}) = gp(y_i^t)\}$. Similar to Bertinetto et al. (2020); Garg et al. (2022a), we also report the continual distance to the Lowest Common Ancestor (LCA) that captures the mistake's hierarchical severity. For the wrong predictions, LCA distance reports the average number of edges between the predicted node and the LCA of the predicted and ground-truth nodes. LCA distance reveals how hierarchically far off the inaccurate predictions are, considering the joint class-instance hierarchy as the ground truth. Following the 3rd CLVision challenge (Verwimp et al., 2023) and the SSLAD competition (Pellegrini et al., 2022)), all continual hierarchical metrics are calculated as the average mean over all the tasks. Here, we take the continual instance-level accuracy as an example. Let $Acc^{ij}_{instance} \in [0, 1]$ denote the instance-level classification accuracy evaluated on the test set of the i-th task after incremental learning of the j-th task. The average mean instance-level accuracy is defined as $\texttt{Accuracy}_{\texttt{instance-level}} = \frac{1}{T^2}\sum_{j=1}^{T}\sum_{i=1}^{T} Acc^{ij}_{instance}$, where T denotes the number of all tasks. We use the same formulation for average mean class-level accuracy and superclass-level accuracies. We also report the per-task accuracies at the end of the last task.

4 HyperCLIC

In this section, we present our method for continual learning of instances and classes using hyperbolic geometry. Our goal is to continually learn hierarchy-aware representations, enabling classification at different levels of granularity: instance-, class-, and superclass-level. Our method consists of two stages. The objective of the first stage (Section 4.1) is to obtain a set of hyperbolic prototypes (Algorithm 1), which are later used in the second stage (Section 4.2) for the classification loss (Algorithm 2). Figure 2 illustrates the two main components of HyperCLIC: First, we embed the class-instance hierarchy into hyperbolic space using Poincaré embeddings and entailment cones, leveraging hyperbolic space's ability to model hierarchical relationships. Second, we perform continual hyperbolic alignment between visual inputs and the embedded hierarchy. We apply a hyperbolic prototype-based loss for classifying new instances and a hyperbolic distillation loss to maintain the consistency of embeddings for previously seen instances, ensuring that the model respects the hierarchical structure during continual learning. Code is available at this link.

4.1 Embedding class-instance hierarchies in hyperbolic space

Given the class-instance tree hierarchy $\mathcal{T}$, our goal is to embed the symbolic tree representation *a priori* into a hyperbolic embedding space that incorporates the hierarchical relations between classes and from classes to instances. We define the hyperbolic manifold using the Poincaré ball model (Nickel & Kiela, 2017), as it is well-suited for gradient-based optimization. More formally, let $\mathbb{B}^d_c = \{\mathrm{z} \in \mathbb{R}^d | c\|\mathrm{z}\|^2 < 1\}$ be the open d-dimensional unit ball, where $||.||$ denotes the Euclidean norm, and c denotes the curvature. The Poincaré ball model corresponds to the Riemannian manifold $(\mathbb{B}^d_c, g^{\mathbb{B}}_{\mathrm{z}})$ with the Riemannian metric tensor $g^{\mathbb{B}}_{\mathrm{z}} = 4(1 - c\|\mathrm{z}\|^2)^{-2}\mathbf{I}_d$.

Let $d_{\mathcal{T}}(v_i, v_j)$ denote the graph distance between two nodes $v_i, v_j \in V$ based on their hierarchical relations. Also, let $d_{\mathbb{B}}(p_i, p_j)$ denote the hyperbolic distance between two points $p_i, p_j \in \mathbb{B}^d$ in the Poincaré ball. We seek to obtain a set of prototypes $P = \{p_i\}_{i=1}^{|V|}$ corresponding to $V = \{v_i\}_{i=1}^{|V|}$ such that $d_{\mathbb{B}}(p_i, p_j) \propto d_{\mathcal{T}}(v_i, v_j)$, *i.e.,* the hyperbolic distance $d_{\mathbb{B}}$ is proportional to the edge distances in graph $\mathcal{T}$. The hyperbolic distance $d_{\mathbb{B}}$ between two points $p_1, p_2 \in \mathbb{B}^d$ is given by the following equation:

$$d_{\mathbb{B}}(p_1, p_2) = \frac{2}{\sqrt{c}} \operatorname{arctanh}(\sqrt{c}||-p_1 \oplus_c p_2||). \tag{1}$$

where $\langle p_1, p_2 \rangle$ denotes the inner product of two vectors p_1 and p_2 and $\oplus$ denotes the Möbius addition given by:

$$p_1 \oplus_c p_2 = \frac{(1 + 2c\langle p_1, p_2\rangle + c||p_2||^2)p_1 + (1 - c||p_1||^2)p_2}{1 + 2c\langle p_1, p_2\rangle + c^2||p_1||^2||p_2||^2} \tag{2}$$

We minimize the loss function $\mathcal{L}_{Poincaré}$ defined by Nickel & Kiela (2017). Let $\mathcal{R} = \{(u, v)\}$ denote the set of transitive closures in graph $\mathcal{T}$, meaning there is a path from node u to v. Ganea et al. (2018a) define $\mathcal{R}$ as entailment relations, where v entails u, or equivalently, that u is a subconcept of v. $\mathcal{L}_{Poincaré}$ encourages semantically similar objects to be close in the embedding space according to their Poincaré distance:

(3)

$\mathcal{N}(u) = \{v|(u, v) \notin \mathcal{R}\} \cup \{u\}$ denotes the set of negative examples for u. Negative examples $\mathcal{N}(u)$ include all nodes v that do not entail u. While the Poincaré loss results in hyperbolic prototypes P in tree-shaped regions on $\mathbb{B}^d$, there are no guarantees of entailment, *i.e.,* of a partial order relationship that requires the region of each subtree to be fully covered by their parent tree. Therefore, following Ganea et al. (2018a), we apply a max-margin entailment loss $\mathcal{L}_{Entailment}$ on the extracted Poincaré embeddings P, to enforce entailment regions:

$$\mathcal{L}_{Entailment} = \sum_{(u,v)\in\mathcal{R}} E(u, v) + \sum_{(u',v')\in\mathcal{N}} max(0, \gamma - E(u', v')). \tag{4}$$

The energy function $E(u, v) := \max(0, \Xi(u, v) - \psi(v))$ measures how far point u from belonging to the entailment cone $\psi(v)$ is. The first term encourages u to be part of the entailment cone $\psi(v)$ for $(u, v) \in \mathcal{R}$. The second term pushes negative samples $(u', v') \in \mathcal{N}$ angularly away for a minimum margin $\gamma > 0$ if they don't share an entailment cone. For full details of Equation 4, we refer to Ganea et al. (2018a).

We observe that the entailment loss tends to bring the prototypes, especially those of the instances V_I, too close to each other. To counteract this, we apply a separation loss $\mathcal{L}_S$, similar to the approach in Long et al. (2020), which ensures that all prototypes P are adequately separated.

$$\mathcal{L}_S(P) = \vec{1}^T(\bar{P}\bar{P}^T - I)\vec{1}, \tag{5}$$

where $\bar{P}$ denotes the vector-wise l_2-normalization of P. The proposed loss function minimizes the cosine similarity between any two prototypes. Algorithm 1 summarizes the first stage of HyperCLIC, detailing the sequential application of the three losses that result in the hyperbolic prototypes. After obtaining the prototypes for all nodes in the tree $\mathcal{T}$, we only use the prototypes $P = \{P_y\}_{y=1}^{|V_I|}$ corresponding to the instance (leaf) nodes $V = \{v_y\}_{y=1}^{|V_I|}$ below.

4.2 Continual Hyperbolic Learning

Our proposed hyperbolic continual learner draws inspiration from the core design choices of iCaRL (Rebuffi et al., 2017), the best-performing model for instance-level classification on the EgoObjects dataset according to Pellegrini (2022). We use a backbone $\varphi(.; \theta_t)$ to extract features from a training sample x_i, where θ_t denotes the model parameters at timestep t. The extracted features form a Euclidean representation $\varphi(x_i; \theta_t)$. We assume that the backbone output is in the tangent space $T_x\mathcal{M}$, while the extracted prototypes from Section 4.1 are in the hyperbolic space $\mathcal{M}$. Thus, we need to project the Euclidean representation to the hyperbolic space $\mathcal{M}$ through an exponential map, which embeds visual representation into the hyperbolic space where the hierarchy of classes and instances are embedded as prototypes:

$$\mathrm{z}_i^t = \exp_0\left(\varphi(\mathrm{x_i}; \theta^t)\right), \qquad \text{where: } \exp_0^c(\mathrm{x}) = \tanh\left(\sqrt{c}\|\mathrm{x}\|\right) \cdot \frac{\mathrm{x}}{\sqrt{c}\|\mathrm{x}\|}. \tag{6}$$

The exponential map definition is borrowed from (Ganea et al., 2018b), where c denotes the curvature of the hyperbolic space. A higher c indicates a more curved space. Here, $\mathrm{z_i}^t$ is the hyperbolic representation of $\varphi(x_i; \theta_t)$. Our goal is to minimize the hyperbolic distance of representation z with its instance prototype P_y. Thus, we define the hyperbolic

Table 1: **Experimental results on EgoObjects** with a ResNet34 backbone. HyperCLIC outperforms all methods with and without pretraining. Methods marked with ♯ are significantly tested against HyperCLIC at $p < 0.05$ (See A.3).

	From scratch					Pretrained				
	Accuracy ↑			LCA ↓	Forgetting ↓	Accuracy ↑			LCA ↓	Forgetting ↓
	Instance	Class	Superclass			Instance	Class	Superclass		
Naive	0.44	1.07	1.58	5.74	10.38	6.06	15.55	18.24	4.70	93.03
EWC	0.22	0.66	1.42	5.26	10.38	6.07	15.77	18.37	4.74	92.83
iCaRL ♯	20.05	21.39	22.24	5.45	10.57	81.63	87.02	87.81	3.89	**3.77**
CoPE	3.14	4.45	4.91	5.63	25.38	37.15	49.89	52.51	4.22	32.40
GDumb	0.50	1.27	1.88	5.50	5.87	61.51	71.00	72.82	4.02	18.22
DER ♯	19.59	20.59	21.14	5.61	35.39	80.00	84.40	85.20	4.28	10.59
HyperCLIC ♯	**41.76**	**45.91**	**48.04**	**4.93**	**4.17**	**84.81**	**91.94**	**92.67**	**2.99**	7.08

logit $h(\mathrm{z}, y)$ as the negative hyperbolic distance of vector representation z and all prototypes y. The conditional probability $p(y_i|\mathrm{z}_i^t)$ can be derived by the softmax of the hyperbolic logit:

$$p(y_i|\mathrm{z}_i^t) = \frac{e^{h(z_i^t, y_i)}}{\sum_{j=1}^{|C|} e^{h(z_i^t, y_j)}}, \qquad \text{where: } h(\mathrm{z}, y) = -\frac{d_{\mathbb{B}}(\mathrm{z}, P_y)}{\tau}. \tag{7}$$

The temperature parameter τ controls the entropy of the probability distribution while preserving the relative ranks of each class. We can make the probability distribution more peaked or smoother by adjusting this parameter.
Once the hyperbolic logits are calculated, we can compute the classification loss as the cross entropy between the hyperbolic logits and the targets:

$$\mathcal{L}_{cls} = -\frac{1}{|\mathcal{D}^t|} \sum_{(x_i, y_i) \in \mathcal{D}^t} \sum_{i=1}^{|C|} y_i \cdot \log\left(\frac{e^{h(z_i^t, y_i)}}{\sum_{j=1}^{|C|} e^{h(z_i^t, y_j)}}\right). \tag{8}$$

While the classification loss ensures that the new classes learn their representation, the ultimate goal of class-incremental learning is to continually learn a model that works both for the old and the new classes. Formally, the model should not only acquire the knowledge from the current task $\mathcal{D}^t$ but also preserve the knowledge from former tasks $\mathcal{D}^{b<t}$. We use a hyperbolic distillation loss to ensure that the model predicts the same hyperbolic logits for the old classes $\mathcal{D}^{b<t}$ at time t as time $t-1$. Following Rebuffi et al. (2017), we keep a copy of the model parameters at time $t-1$ as θ^{t-1} and define the probability distribution at time $t-1$ as $p(y_i|\mathrm{z}_i^{t-1})$ where $(x_i, y_i) \in \mathcal{D}^{b<t}$:

$$p(y_i|\mathrm{z}_i^{t-1}) = \frac{e^{h(z_i^{t-1}, y_i)}}{\sum_{j=1}^{|C|} e^{h(z_i^{t-1}, y_j)}}. \tag{9}$$

The hyperbolic distillation loss is calculated as the cross-entropy loss between the probability distribution at time t and $t-1$:

$$\mathcal{L}_{distil} = -\frac{1}{|\mathcal{D}^{b<t}|} \sum_{(x_i, y_i) \in \mathcal{D}^{b<t}} \sum_{i=1}^{|C^{b<t}|} \left(\frac{e^{h(z_i^{t-1}, y_i)}}{\sum_{j=1}^{|C^{b<t}|} e^{h(z_i^{t-1}, y_j)}}\right) \cdot \log\left(\frac{e^{h(z_i^t, y_i)}}{\sum_{j=1}^{|C^{b<t}|} e^{h(z_i^t, y_j)}}\right). \tag{10}$$

The final loss of the second stage is $\mathcal{L} = \mathcal{L}_{cls} + \mathcal{L}_{distil}$ following Rebuffi et al. (2017). Algorithm 2 summarizes the second stage of HyperCLIC, where the hyperbolic prototypes from the first stage are used to classify new classes at the current task and distill hyperbolic logits from previously seen classes. Samples from old classes $\mathcal{D}^{b<t}$ are selected at the end of each task by the herding strategy (Welling, 2009), which is a commonly used strategy aiming to select the most representative samples of each class. These exemplars are saved in memory and are representative data points of each known instance class. In addition to distillation loss, the exemplars are also used during inference. During inference, the closeness to exemplars determines the final prediction for a given data point. We perform the nearest mean of exemplar classification following Rebuffi et al. (2017): $y_i^* = \arg\min_{y=1,\ldots,n_I} \|\varphi(\mathrm{x_i}) - \mu_y\|$, where μ_y denotes the mean of exemplars for the instance class y and n_I denotes the number of instance classes. The exemplars and their means could be calculated in hyperbolic space, however, we observe that the Euclidean representations are already aligned with the hierarchy and conclude that there is no need for an extra hyperbolic computation. Overall, our method aligns classification and distillation losses with hyperbolic representations of a fixed hierarchy, leveraging the class-instance hierarchy with minor modifications to existing continual learning methods. This alignment allows continual classification at multiple levels of granularity such as instance and class-level.

5 RESULTS

Dataset We focus on EgoObjects (Zhu et al., 2023) since it is the only large-scale class-incremental dataset with a significant number of instances *and* classes and a non-trivial hierarchy, reflecting real-world complex hierarchical structures. Core50 dataset (Lomanco & Maltoni, 2017) is also an instance-level dataset, but is a toy dataset with only 10 classes with 5 instances each, resulting in minimal differences between methods. We see a great potential for additional large instance-level continual datasets due to the real-world relevance, but there is unfortunately a lack of large-scale instance-level continual datasets. The EgoObjects benhcmark (Zhu et al., 2023), first introduced at the 3rd CLVISION Challenge (Pellegrini et al., 2022), represents a challenging benchmark for continual learning, particularly because of the instance-level object understanding with 1110 unique instances across 277 classes. The objects follow an imbalanced long-tailed distribution with varying clutter, occlusion, lighting, and backgrounds. The order of classes follows scenarios of ever-evolving environments with the reoccurance of previously seen objects (Hemati et al., 2025). This dataset comprises a stream of 15 tasks, each created by cropping the main object from egocentric videos with each task including 74 instances. Since the test set labels are not provided in the challenge, we split the training set into training (80%), testing (10%), and validation (10%) subsets. Following the challenge convention, we divide the dataset into non-overlapping sets of `gaia_ids`, which are identifiers for each unique video clip. For reproducibility purposes, we have provided the code and metadata including the hierarchy and the train, test and validation sets at this link.

Hierarchies For the EgoObjects (Zhu et al., 2023) dataset, we construct a hierarchy using WordNet (Fellbaum, 2010), a comprehensive lexical database of the English language. We match each class in the dataset with the most frequent noun synset in WordNet. To find the path from the leaf nodes to the root node, we iteratively choose the hypernym with the shortest path to the root. If this path does not include the `physical_entity.n.01` node, we select the next shortest path that does. We manually add classes that do not match any synsets to the hierarchy. Categories without any instances (91 out of 277) are removed. We also remove nodes with only one child, except for parents of leaf nodes. The resulting unbalanced hierarchy has a maximum of 7 instances per category, a minimum of 1, and a depth of 12. Our automated hierarchy extraction method can be adapted to other datasets. The hierarchy is provided with the code at this link to enable reproducibility.

Implementation details For HyperCLIC EgoObjects experiments, we train a ResNet34 backbone for 3 epochs following Pellegrini (2022), with a batch_size of 90, and a learning rate of 0.01 for 15 tasks. The memory size is 3500 according to the challenge. The pretrained models are pretrained with `ResNet34_Weights.IMAGENET1K_V1`, `Wide_ResNet50_2_Weights.IMAGENET1K_V2` and `RegNet_X_16GF_Weights.IMAGENET1K_V2`. In all datasets, the curvature of the Poincaré model (`PoincaréBallExact` Kochurov et al. (2020)) is 1. The hyperbolic prototypes are 64-dimensional using Ganea et al. (2018a) with 150 Poincaré epochs and 50 entailment epochs, plus separation following Long et al. (2020) with a learning rate of 1.0 for 500 epochs. For all experiments, we choose the hyperparameters of our method with minimal hyperparameter tuning for fair comparison. Following hyperbolic learning literature, we set the temperature parameter τ to a common value of 0.1 (Ibrahimi et al., 2024a; Long et al., 2020; Sinha et al., 2024). Parameter λ was fixed at 0.5 to balance distillation and classification objectives equally. We show that the results can be improved with better backbones. For consistency, we applied the same hyperparameters (optimized for 15-task scenarios) across all evaluations. As shown in Table 2, this leads to some performance variations - for instance, DER achieves better results than HyperCLIC on the 6-task scenario. All methods would probably benefit from extensive tuning but that was not explored in the paper.

Baselines We evaluate HyperCLIC against four canonical CIL methods representing key strategies: EWC (Kirkpatrick et al., 2017) (regularization-based), iCaRL (Rebuffi et al., 2017) and GDumb (Prabhu et al., 2020) (replay-based), and DER (Yan et al., 2021) (architecture expansion). Additionally, we compare to CoPE (De Lange & Tuytelaars, 2021), an online prototype-based approach well-suited for EgoObjects, and naive fine-tuning. The baseline methods were designed without hierarchical information, and there is no non-trivial way to integrate hierarchical structure into their existing frameworks. This underlines the importance of our proposed method and the fact that other continual learning methods could benefit from including the hierarchical information in future research. Comparison to Gao et al. (2023) was unfortunately not possible due to the unavailability of their code. Our goal is to advocate joint instance- and class-level continual learning and hyperbolic embeddings' potential to enrich hierarchical representations in standard continual learning scenarios. We therefore focus on the most well-known approaches in continual learning. We believe that generalizing recent instance-level approaches to our task is an interesting future

Table 2: **Experimental results on EgoObjects with 6 and 37 tasks** from scratch with a ResNet34 backbone.

	Instance ↑		Class ↑		Superclass ↑		LCA ↓		Forgetting ↓	
	6	37	6	37	6	37	6	37	6	37
Naive	02.53	00.21	03.48	1.13	04.11	1.74	5.73	5.54	22.10	10.60
EWC	02.47	00.25	03.51	1.31	04.52	1.31	5.62	7.69	21.99	11.52
iCaRL	23.56	17.46	24.74	18.74	25.69	19.57	5.41	5.48	6.60	12.22
GDumb	00.56	00.71	01.24	1.75	01.36	2.39	5.59	5.30	5.37	6.46
DER	**36.01**	2.05	**36.99**	2.85	37.75	3.34	5.42	5.74	12.70	45.76
HyperCLIC	34.09	**39.86**	36.71	**47.18**	**38.06**	**49.81**	**5.12**	**4.48**	**00.26**	**5.73**

research direction. Our implementations are based on Lomonaco et al. (2021). ICaRL is particularly relevant as it is the best-performing model for instance-level classification on EgoObjects (Pellegrini, 2022).

Comparison to existing methods Table 1 reports the results of different baselines on the EgoObjects dataset with 15 tasks. If trained from scratch, HyperCLIC achieves a significantly higher instance-level accuracy (41.76%), class-level accuracy (45.91%), and superclass-level accuracy (48.04%) compared to all baselines. The closest competitor is iCaRL (Rebuffi et al., 2017) with an instance-, class-, and superclass-level accuracy of 20.05%, 21.39%, and 22.24%, respectively, which is less than half of HyperCLIC 's performance. This demonstrates HyperCLIC's strength in maintaining performance across different levels of granularity. HyperCLIC shows a lower LCA value (4.93) indicating that the inaccurate predictions are less hierarchically severe compared to other baselines. The second-best is EWC (Kirkpatrick et al., 2017) with 5.26. HyperCLIC also shows the lowest forgetting rate (4.17%), indicating better retention of learned knowledge. The low scores of baselines is due to the large number of instances and the long-tailed distribution. They fail to differentiate between instances in the EgoObjects dataset even in one task, because of the challenging nature of the dataset. In general, instance-level continual learning faces different challenges compared with class-level continual learning. For the pretrained scenario, HyperCLIC leads with the instance-level accuracy of 84.81%, followed by iCaRL (Rebuffi et al., 2017) with 81.63%, and DER (Yan et al., 2021) with 80%. DER is a strong non-transformer-based continual baseline. Across both trained-from-scratch and pretrained scenarios, HyperCLIC consistently outperforms all baselines on every metric. As shown in Table 2, HyperCLIC achieves the highest performance in the challenging 37-task setting and ranks second in instance- and class-level accuracy for 6 tasks. The performance differences between DER, HyperCLIC, and iCaRL on EgoObjects in Table 2 can be attributed to their distinct approaches to continual learning. DER demonstrates stronger performance in the 6-task scenario due to its inherent robustness with fewer tasks, though this advantage diminishes with the 37-task setup where its performance declines more significantly. HyperCLIC maintains more stable results across different task quantities thanks to its hierarchical structure, which provides consistent representation learning despite being slightly outperformed by DER in the 6-task case. Meanwhile, iCaRL shows greater sensitivity to task quantity variations, with performance dropping for both 6 and 37 tasks compared to the 15-task baseline, though its smaller performance gap between 6 and 37 tasks suggests potential for improvement through hyperparameter optimization. All methods in Table 2 used identical hyperparameters as Table 1, indicating that task-specific tuning could further enhance their results. HyperCLIC's excelling in instance-, class-, and superclass-level accuracy while maintaining lower LCA and minimal forgetting, HyperCLIC demonstrates its ability to learn hierarchically-aware representations while preserving knowledge from previous tasks.

Given that iCaRL (Rebuffi et al., 2017) has the highest performance after HyperCLIC, we use it as the primary comparison for evaluating our method in subsequent experiments. Table 4 illustrates the instance-level accuracy for each task (T1 to T15) after the completion of all tasks. In both non-pretrained and pretrained models, iCaRL (Rebuffi et al., 2017) demonstrates higher stability but at the cost of not learning effective representations for new tasks, thereby compromising its performance on recent tasks to retain knowledge from previous ones. We can also observe this behavior in Table 1. In contrast, our method not only preserves knowledge from prior tasks but also achieves higher accuracy on the latest tasks compared to the baseline.

Class-level errors Figure 3 compares the class-level confusion matrix for incorrectly predicted instances between iCaRL and HyperCLIC, alongside the distances of hyperbolic prototypes. In this matrix, the squares represent children of the same parent node, and larger squares encompass multiple subtrees. The aim of this experiment is to demonstrate that even when instances are misclassified, HyperCLIC's class-level predictions still follow the hierarchical structure. As shown, iCaRL's class-level predictions are evenly distributed, while HyperCLIC's predictions are primarily concentrated along the diagonal. Additionally, a similar hierarchical organization is observed in HyperCLIC when compared with the pairwise hyperbolic prototype distances, represented by matching squares. This indicates that HyperCLIC maintains the hierarchical structure, even when making

Table 3: **Balancing the effect of classification and distillation losses in EgoObjects dataset.** Equally weighting the losses yields the highest performance in HyperCLIC.

λ	Accuracy ↑			LCA ↓	Forgetting ↓
	Instance	Class	Superclass		
0.1	35.33	39.71	42.09	4.90	7.28
0.3	37.54	42.05	44.51	4.83	6.18
Ours	41.76	45.91	48.04	4.93	4.17
0.7	38.02	41.56	43.38	4.92	-0.59
0.9	24.49	26.55	27.83	5.32	-4.92

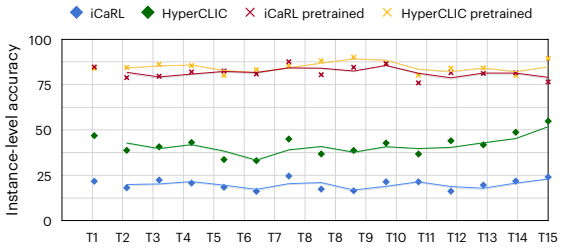


Table 4: **The final per-task accuracies and moving average on EgoObjects**. HyperCLIC outperforms iCaRL by maintaining prior knowledge while delivering higher accuracy on new tasks.

incorrect predictions, resulting in less severe errors. Figure 3 is the qualitative demonstration of the quantitative LCA metric. This figure shows the class-level predictions only for the wrong instance-level predictions and highlights the hierarchical structure of the mistakes of HyperCLIC. LCA measures the number of edges between the incorrect prediction and the lowest common ancestor of the ground-truth and prediction. Intuitively, if an object is incorrectly predicted at instance level but correctly at class level, the LCA is equal to 1. If an object is incorrectly predicted at instance level but correctly at superclass level, the LCA is equal to 2 instead.

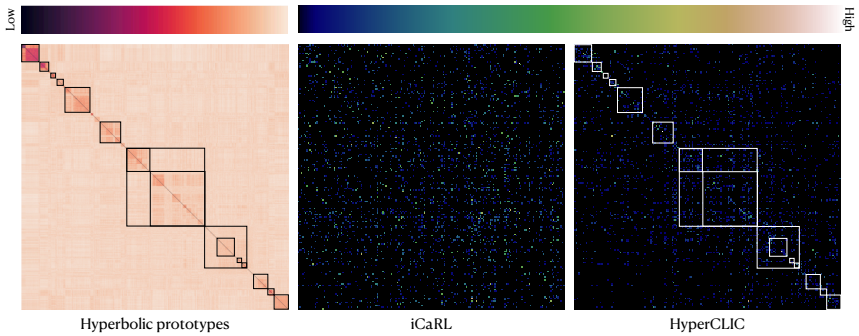


Figure 3: **Left:** the pair-wise distances of the instance-level hyperbolic prototypes. **Middle & right:** the class-level predictions only for the wrong instance-level predictions. The squares highlight the hierarchical structure of HyperCLIC mistakes compared with iCaRL and its similarity to the original hierarchy.

Qualitative examples: success and failure cases Figure 4 presents several images from the test set and compares the instance and class-level predictions of our method against the baseline. In the first row and the first column, both methods easily make correct instance-level predictions. Whereas, in the far-right column in the first row, it is challenging for both methods, as it depicts food items in a drawing, leading both to predict unrelated instances and classes. The middle examples reveal that when HyperCLIC makes an incorrect instance-level prediction, the class-level prediction remains hierarchically close. HyperCLIC makes more instance-level mistakes, while correctly classifying at class level. Another distinction of HyperCLIC is that class-level mistakes are hierarchically correct. For example, it might mistake a "Christmas bush" for a "house plant" or a "bottle" for a "mug", whereas, iCaRL mistakes "basket ball" for a "bread knife" or a "wine glass" for an "orange". This suggests that by incorporating hierarchical information during training, HyperCLIC reduces the severity of hierarchical errors.

Temperature In the second stage of HyperCLIC, one of the key hyperparameters that significantly impacts the continual learning of new classes in the classification loss is the temperature. The temperature, τ, controls the smoothness of the probability distribution derived from the pairwise distances of the hyperbolic prototypes. In hyperbolic literature (Ibrahimi et al., 2024b; Long et al., 2020), τ is commonly set to 0.1. Our results, as shown in Table 5, indicate that HyperCLIC is highly sensitive to the choice of temperature, especially when trained from scratch compared to using a pretrained model. The best performance is consistently achieved with a temperature of 0.1 in both scenarios. When the probability distribution is either too peaked or too smooth, the model struggles to effectively distinguish between classes.

Distillation loss A key component of our method is the distillation loss, which ensures that the model retains hyperbolic knowledge from previous tasks. To evaluate this, we tested three different loss functions: Kullback-Leibner (KL) divergence, Mean Squared Error (MSE), and cross-entropy loss. Table 6 presents the results for both pretrained and from-scratch scenarios. KL divergence shows the lowest forgetting rates, at -1.40% and -6% respectively, for from-scratch and pretrained scenarios. However, it performs the worst in terms of hierarchical metrics and instance

Table 5: **The effect of different temperatures on HyperCLIC in EgoObjects.** Our setting with temperature of 0.1 is highlighted in gray. Our method is more sensitive to the temperature in the from-scratch setting.

	From scratch					Pretrained				
	Instance	Class	Superclass	LCA	Forgetting	Instance	Class	Superclass	LCA	Forgetting
0.01	26.14	28.26	29.18	5.38	-1.81	77.79	84.90	85.64	3.92	8.06
0.05	11.79	12.93	13.78	5.54	4.52	82.21	90.02	91.16	2.97	6.67
0.09	38.21	42.59	44.44	4.83	3.54	82.03	89.93	91.13	2.91	5.21
Ours	41.76	45.91	48.04	4.93	4.17	84.81	91.94	92.67	2.99	7.08
0.3	19.76	24.07	27.22	4.94	11.82	79.22	88.76	89.88	2.88	7.70
0.5	16.35	20.77	23.68	4.97	9.11	76.80	87.35	88.72	2.74	6.34
1.0	12.67	16.52	19.21	5.03	10.39	71.86	85.35	87.21	2.62	6.47

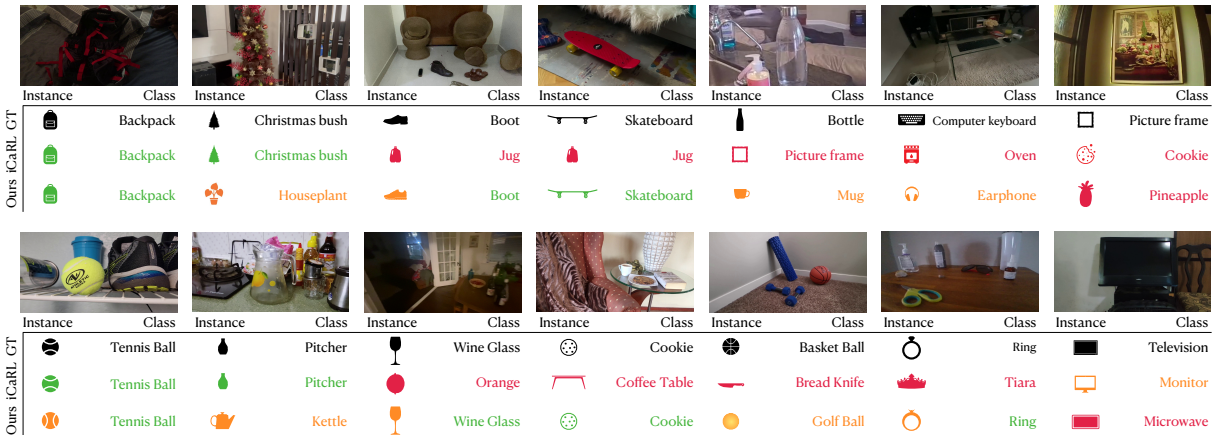


Figure 4: **Qualitative examples from EgoObjects** comparing instance and class-level predictions for ground truth (1st row), iCaRL (2nd row), and our method (3rd row). Green indicates correct predictions, while red and orange denote severe and less severe hierarchical errors, respectively. HyperCLIC makes less severe errors compared to iCaRL.

accuracy, suggesting it disrupts the balance between plasticity and stability by favoring stability at the expense of plasticity. Cross-entropy loss performs the best across both scenarios, which is why our method is based on this loss function. There is also a more notable difference between MSE and cross-entropy when training from scratch compared to the pretrained scenario.

Balancing classification and distillation losses The continual learning objective in the second stage of HyperCLIC combines classification and distillation losses, following iCaRL. To evaluate the impact of each loss term, we use a balancing factor, λ, as shown in the loss function: $\mathcal{L} = \lambda \cdot \mathcal{L}_{distil} + (1-\lambda) \cdot \mathcal{L}_{cls}$. By varying λ, we assess the influence of classification and distillation losses on the model's performance. Table 3 presents the results for different λ values. Our findings indicate that a fully balanced loss achieves the best performance across both instance-level accuracy and hierarchical metrics. The balanced weighting ($\lambda = 0.5$) emerges as optimal because it maintains numerical equilibrium between the two losses. Emphasis on distillation ($\lambda > 0.5$) compromises learning new tasks, while

Table 6: **EgoObjects results with different distillation losses** with a ResNet34 backbone. Cross-entropy loss consistently outperforms other distillation losses in both scenarios.

	From scratch					Pretrained				
	Instance	Class	Superclass	LCA	Forgetting	Instance	Class	Superclass	LCA	Forgetting
KL divergence	32.60	35.30	36.95	5.13	-1.40	49.76	62.45	65.46	3.75	-6.00
MSE	36.09	40.33	42.53	4.94	8.18	84.38	91.21	92.33	2.92	7.84
Cross-entropy	41.76	45.91	48.04	4.93	4.17	84.11	91.61	92.54	2.96	7.08

Table 7: **Comparison of iCaRL and HyperCLIC on EgoObjects with various backbones pretrained on ImageNet-1K.** HyperCLIC consistently outperforms iCaRL regardless of the architecture. This demonstrates that HyperCLIC is adaptable to any backbone and, when paired with advanced models, enhances joint continual learning of instances and classes.

	iCaRL					HyperCLIC				
	Instance	Class	Superclass	LCA	Forgetting	Instance	Class	Superclass	LCA	Forgetting
WideResNet50	82.17	87.46	88.08	4.02	3.42	86.50	94.17	94.61	2.58	6.01
RegNetX_16GF	78.63	86.64	87.58	3.55	5.10	87.22	94.11	95.01	2.59	5.99
ResNet34	81.63	87.02	87.81	3.89	3.77	84.81	91.94	92.67	2.99	7.08
ViTB/16	80.61	89.02	89.83	3.27	1.94	88.61	94.62	95.36	2.67	4.01

over-prioritizing classification ($\lambda < 0.5$) leads to catastrophic forgetting of previous knowledge. This observation is consistent with iCaRL's formulation where the unweighted sum of classification and distillation losses proves most effective, suggesting that neither objective should dominate during optimization. This highlights the importance of giving equal weight to both losses to ensure that the model can effectively learn new classes while retaining knowledge of previously learned classes.

Backbones All results reported thus far utilize the ResNet34 backbone. Table 7 compares our method with the leading baseline (iCaRL), using various pretrained backbones. The findings indicate that HyperCLIC consistently surpasses the baseline across the hierarchical metrics when using WideResNet50, RegNetX, ResNet34 and ViTB/16 as the backbone architectures. Notably, HyperCLIC achieves the highest performance with the ViTB/16 backbone, attaining instance-, class-, and superclass-level accuracies of 88.61%, 94.62%, and 95.36%, respectively, compared to the best iCaRL results for WideResNet, which are 82.17%, 87.46%, and 88.08%. Although HyperCLIC improves the LCA distance by nearly one edge, leading to better hierarchical mistakes, it shows a higher forgetting rate. These results suggest that our method, particularly when combined with advanced models, has the potential to significantly enhance the joint continual learning of instances and classes. We further analyze the impact of the number of fine-tuned layers in HyperCLIC compared to Euclidean-based methods (iCaRL) in Appendix A.2.

6 Conclusion and Discussion

Instance-level continual learning addresses the challenging task of recognizing and remembering specific instances of object classes in an incremental setup, where new instances appear over time. This approach forms a more fine-grained challenge than conventional continual learning, which typically focuses on incremental discrimination at the class level. In this paper, we introduced a method for continually learning at both instance and class levels, arguing that real-world continual understanding requires recognizing samples at multiple layers of granularity. We observed that classes and instances form a hierarchical structure that can be leveraged to enhance learning at both levels. To this end, we proposed HyperCLIC, a hyperbolic continual algorithm designed for jointly learning instances and classes. We introduced continual hyperbolic classification and hyperbolic distillation, which embed the hierarchical relationships. Our experiments demonstrated that HyperCLIC operates effectively at multiple levels of granularity. We conducted ablations on different distillation losses, backbone architectures, and pretrained models. Our qualitative analysis provided evidence that HyperCLIC makes less hierarchically severe mistakes. HyperCLIC enables real-world continual understanding, where recognizing and remembering both instances and classes over time is crucial.

Our approach shares conceptual similarities with exemplar-free prototype-based approaches in using compressed representations to mitigate forgetting. The key distinction is that we maintain both exemplars and prototypes to preserve hierarchical relationships—exemplars help anchor fine-grained instance-level features, while hyperbolic prototypes capture the class hierarchy. We believe that the geometric properties of hyperbolic space can benefit exemplar-free approaches in several ways, for instances by including a hierarchical prototype alignment and we see this as an intriguing future research direction.

References

Rahaf Aljundi, Min Lin, Baptiste Goujaud, and Yoshua Bengio. Gradient based sample selection for online continual learning. *NeurIPS*, 2019.

Phil Ammirato. *Recognizing Fine-Grained Object Instances for Robotics Applications*. PhD thesis, The University of North Carolina at Chapel Hill, 2019.

Mina Ghadimi Atigh, Julian Schoep, Erman Acar, Nanne Van Noord, and Pascal Mettes. Hyperbolic image segmentation. In *CVPR*, 2022.

Gregor Bachmann, Gary Bécigneul, and Octavian Ganea. Constant curvature graph convolutional networks. In *ICML*, 2020.

Jihwan Bang, Heesu Kim, YoungJoon Yoo, Jung-Woo Ha, and Jonghyun Choi. Rainbow memory: Continual learning with a memory of diverse samples. In *CVPR*, 2021.

Eden Belouadah and Adrian Popescu. Il2m: Class incremental learning with dual memory. In *ICCV*, 2019.

Luca Bertinetto, Romain Mueller, Konstantinos Tertikas, Sina Samangooei, and Nicholas A Lord. Making better mistakes: Leveraging class hierarchies with deep networks. In *CVPR*, 2020.

Ali Borji, Saeed Izadi, and Laurent Itti. ilab-20m: A large-scale controlled object dataset to investigate deep learning. In *CVPR*, 2016.

Pietro Buzzega, Matteo Boschini, Angelo Porrello, Davide Abati, and Simone Calderara. Dark experience for general continual learning: a strong, simple baseline. *NeurIPS*, 2020.

Ines Chami, Zhitao Ying, Christopher Ré, and Jure Leskovec. Hyperbolic graph convolutional neural networks. *NeurIPS*, 2019.

Arslan Chaudhry, Puneet K Dokania, Thalaiyasingam Ajanthan, and Philip HS Torr. Riemannian walk for incremental learning: Understanding forgetting and intransigence. In *ECCV*, 2018a.

Arslan Chaudhry, Marc'Aurelio Ranzato, Marcus Rohrbach, and Mohamed Elhoseiny. Efficient lifelong learning with a-gem. *arXiv preprint arXiv:1812.00420*, 2018b.

Bike Chen, Wei Peng, Xiaofeng Cao, and Juha Röning. Hyperbolic uncertainty aware semantic segmentation. *T-ITS*, 2023.

Zhiyuan Chen and Bing Liu. *Lifelong machine learning*. Springer, 2018.

Hyunghoon Cho, Benjamin DeMeo, Jian Peng, and Bonnie Berger. Large-margin classification in hyperbolic space. In *AIStat*, 2019.

Seunghyuk Cho, Juyong Lee, and Dongwoo Kim. Hyperbolic vae via latent gaussian distributions. *NeurIPS*, 2024.

Jindou Dai, Yuwei Wu, Zhi Gao, and Yunde Jia. A hyperbolic-to-hyperbolic graph convolutional network. In *CVPR*, 2021.

Shuyang Dai, Zhe Gan, Yu Cheng, Chenyang Tao, Lawrence Carin, and Jingjing Liu. Apo-vae: Text generation in hyperbolic space. *arXiv preprint arXiv:2005.00054*, 2020.

Matthias De Lange and Tinne Tuytelaars. Continual prototype evolution: Learning online from non-stationary data streams. In *ICCV*, 2021.

Matthias De Lange, Rahaf Aljundi, Marc Masana, Sarah Parisot, Xu Jia, Aleš Leonardis, Gregory Slabaugh, and Tinne Tuytelaars. A continual learning survey: Defying forgetting in classification tasks. *TPAMI*, 2021.

Jia Deng, Wei Dong, Richard Socher, Li-Jia Li, Kai Li, and Li Fei-Fei. Imagenet: A large-scale hierarchical image database. In *CVPR*, 2009.

Karan Desai, Maximilian Nickel, Tanmay Rajpurohit, Justin Johnson, and Shanmukha Ramakrishna Vedantam. Hyperbolic image-text representations. In *ICML*, 2023.

Ankit Dhall, Anastasia Makarova, Octavian Ganea, Dario Pavllo, Michael Greeff, and Andreas Krause. Hierarchical image classification using entailment cone embeddings. In *CVPR*, 2020.

Bhuwan Dhingra, Christopher J Shallue, Mohammad Norouzi, Andrew M Dai, and George E Dahl. Embedding text in hyperbolic spaces. *arXiv preprint arXiv:1806.04313*, 2018.

Jiahua Dong, Lixu Wang, Zhen Fang, Gan Sun, Shichao Xu, Xiao Wang, and Qi Zhu. Federated class-incremental learning. In *CVPR*, 2022.

Lars Jelte Doorenbos, Pablo Márquez Neila, Raphael Sznitman, and Pascal Mettes. Hyperbolic random forests. *TMLR*, 2024.

Arthur Douillard, Matthieu Cord, Charles Ollion, Thomas Robert, and Eduardo Valle. Podnet: Pooled outputs distillation for small-tasks incremental learning. In *ECCV*, 2020.

Arthur Douillard, Alexandre Ramé, Guillaume Couairon, and Matthieu Cord. Dytox: Transformers for continual learning with dynamic token expansion. In *CVPR*, 2022.

Itay Evron, Edward Moroshko, Rachel Ward, Nathan Srebro, and Daniel Soudry. How catastrophic can catastrophic forgetting be in linear regression? In *Conference on Learning Theory*, 2022.

C Fellbaum. About wordnet. wordnet. princeton university, 2010.

Octavian Ganea, Gary Bécigneul, and Thomas Hofmann. Hyperbolic entailment cones for learning hierarchical embeddings. In *ICML*, 2018a.

Octavian Ganea, Gary Bécigneul, and Thomas Hofmann. Hyperbolic neural networks. *NeurIPS*, 2018b.

Zhi Gao, Yuwei Wu, Yunde Jia, and Mehrtash Harandi. Curvature generation in curved spaces for few-shot learning. In *ICCV*, 2021.

Zhi Gao, Chen Xu, Feng Li, Yunde Jia, Mehrtash Harandi, and Yuwei Wu. Exploring data geometry for continual learning. In *CVPR*, 2023.

Ashima Garg, Depanshu Sani, and Saket Anand. Learning hierarchy aware features for reducing mistake severity. In *ECCV*, 2022a.

Prachi Garg, Rohit Saluja, Vineeth N Balasubramanian, Chetan Arora, Anbumani Subramanian, and CV Jawahar. Multi-domain incremental learning for semantic segmentation. In *WACV*, 2022b.

Songwei Ge, Shlok Mishra, Simon Kornblith, Chun-Liang Li, and David Jacobs. Hyperbolic contrastive learning for visual representations beyond objects. In *CVPR*, 2023.

Mina Ghadimi Atigh, Martin Keller-Ressel, and Pascal Mettes. Hyperbolic busemann learning with ideal prototypes. *NeurIPS*, 2021.

Yiduo Guo, Bing Liu, and Dongyan Zhao. Online continual learning through mutual information maximization. In *ICML*, 2022a.

Yunhui Guo, Xudong Wang, Yubei Chen, and Stella X Yu. Clipped hyperbolic classifiers are super-hyperbolic classifiers. In *CVPR*, 2022b.

Matthias Hamann. On the tree-likeness of hyperbolic spaces. In *Mathematical proceedings of the cambridge philosophical society*. Cambridge University Press, 2018.

David Held, Sebastian Thrun, and Silvio Savarese. Robust single-view instance recognition. In *IEEE International Conference on Robotics and Automation (ICRA)*, 2016.

Hamed Hemati, Lorenzo Pellegrini, Xiaotian Duan, Zixuan Zhao, Fangfang Xia, Marc Masana, Benedikt Tscheschner, Eduardo Veas, Yuxiang Zheng, Shiji Zhao, et al. Continual learning in the presence of repetition. *Neural Networks*, 2025.

Geoffrey Hinton, Oriol Vinyals, and Jeff Dean. Distilling the knowledge in a neural network. *arXiv preprint arXiv:1503.02531*, 2015.

Jie Hong, Zeeshan Hayder, Junlin Han, Pengfei Fang, Mehrtash Harandi, and Lars Petersson. Hyperbolic audio-visual zero-shot learning. In *ICCV*, 2023.

Saihui Hou, Xinyu Pan, Chen Change Loy, Zilei Wang, and Dahua Lin. Learning a unified classifier incrementally via rebalancing. In *CVPR*, 2019.

Sarah Ibrahimi, Mina Ghadimi Atigh, Nanne Van Noord, Pascal Mettes, and Marcel Worring. Intriguing properties of hyperbolic embeddings in vision-language models. *TMLR*, 2024a.

Sarah Ibrahimi, Mina Ghadimi Atigh, Nanne Van Noord, Pascal Mettes, and Marcel Worring. Intriguing properties of hyperbolic embeddings in vision-language models. *TMLR*, 2024b.

Tobias Kalb, Masoud Roschani, Miriam Ruf, and Jürgen Beyerer. Continual learning for class-and domain-incremental semantic segmentation. In *IEEE IV*, 2021.

Minsoo Kang, Jaeyoo Park, and Bohyung Han. Class-incremental learning by knowledge distillation with adaptive feature consolidation. In *CVPR*, 2022.

Valentin Khrulkov, Leyla Mirvakhabova, Evgeniya Ustinova, Ivan Oseledets, and Victor Lempitsky. Hyperbolic image embeddings. In *CVPR*, 2020.

Mert Kilickaya and Joaquin Vanschoren. Are labels needed for incremental instance learning? In *CVPR*, 2023.

Gyuhak Kim, Changnan Xiao, Tatsuya Konishi, Zixuan Ke, and Bing Liu. A theoretical study on solving continual learning. *NeurIPS*, 2022.

Gyuhak Kim, Changnan Xiao, Tatsuya Konishi, and Bing Liu. Learnability and algorithm for continual learning. In *ICML*, 2023.

James Kirkpatrick, Razvan Pascanu, Neil Rabinowitz, Joel Veness, Guillaume Desjardins, Andrei A Rusu, Kieran Milan, John Quan, Tiago Ramalho, Agnieszka Grabska-Barwinska, et al. Overcoming catastrophic forgetting in neural networks. *Proceedings of the national academy of sciences*, 2017.

Max Kochurov, Rasul Karimov, and Serge Kozlukov. Geoopt: Riemannian optimization in pytorch. *arXiv preprint arXiv:2005.02819*, 2020.

Marc Law, Renjie Liao, Jake Snell, and Richard Zemel. Lorentzian distance learning for hyperbolic representations. In *ICML*, 2019.

Byung Hyun Lee, Okchul Jung, Jonghyun Choi, and Se Young Chun. Online continual learning on hierarchical label expansion. In *ICCV*, 2023.

Janghyeon Lee, Hyeong Gwon Hong, Donggyu Joo, and Junmo Kim. Continual learning with extended kronecker-factored approximate curvature. In *CVPR*, 2020.

Matthias Leimeister and Benjamin J Wilson. Skip-gram word embeddings in hyperbolic space. *arXiv preprint arXiv:1809.01498*, 2018.

Zhizhong Li and Derek Hoiem. Learning without forgetting. *IEEE PAMI*, 2017.

Qi Liu, Maximilian Nickel, and Douwe Kiela. Hyperbolic graph neural networks. *NeurIPS*, 2019.

Shaoteng Liu, Jingjing Chen, Liangming Pan, Chong-Wah Ngo, Tat-Seng Chua, and Yu-Gang Jiang. Hyperbolic visual embedding learning for zero-shot recognition. In *CVPR*, 2020.

V Lomanco and Davide Maltoni. Core50: a new dataset and benchmark for continual object recognition. In *PMLR*, 2017.

Vincenzo Lomonaco, Lorenzo Pellegrini, Andrea Cossu, Antonio Carta, Gabriele Graffieti, Tyler L Hayes, Matthias De Lange, Marc Masana, Jary Pomponi, Gido M Van de Ven, et al. Avalanche: an end-to-end library for continual learning. In *CVPR*, 2021.

Teng Long, Pascal Mettes, Heng Tao Shen, and Cees GM Snoek. Searching for actions on the hyperbole. In *CVPR*, 2020.

David Lopez-Paz and Marc'Aurelio Ranzato. Gradient episodic memory for continual learning. *NeurIPS*, 2017.

Clare Lyle, Zeyu Zheng, Khimya Khetarpal, Hado van Hasselt, Razvan Pascanu, James Martens, and Will Dabney. Disentangling the causes of plasticity loss in neural networks. *arXiv preprint arXiv:2402.18762*, 2024.

Simone Magistri, Joost van de Weijer, Andew D Bagdanov, et al. An empirical analysis of forgetting in pre-trained models with incremental low-rank updates. *arXiv preprint arXiv:2405.18069*, 2024.

Emile Mathieu and Maximilian Nickel. Riemannian continuous normalizing flows. *NeurIPS*, 2020.

Pascal Mettes, Mina Ghadimi Atigh, Martin Keller-Ressel, Jeffrey Gu, and Serena Yeung. Hyperbolic deep learning in computer vision: A survey. *IJCV*, 2024.

M Jehanzeb Mirza, Marc Masana, Horst Possegger, and Horst Bischof. An efficient domain-incremental learning approach to drive in all weather conditions. In *CVPR*, 2022.

Shishir Muralidhara, Saqib Bukhari, Georg Schneider, Didier Stricker, and René Schuster. Cleo: Continual learning of evolving ontologies. In *ECCV*, 2024.

Maximillian Nickel and Douwe Kiela. Poincaré embeddings for learning hierarchical representations. *NeurIPS*, 2017.

Maximillian Nickel and Douwe Kiela. Learning continuous hierarchies in the lorentz model of hyperbolic geometry. In *ICML*, 2018.

Kishan Parshotam and Mert Kilickaya. Continual learning of object instances. In *CVPR*, 2020.

Lorenzo Pellegrini. clvision-challenge-2022 reports. https://github.com/ContinualAI/clvision-challenge-2022/tree/main/reports, 2022.

Lorenzo Pellegrini, Chenchen Zhu, Fanyi Xiao, Zhicheng Yan, Antonio Carta, Matthias De Lange, Vincenzo Lomonaco, Roshan Sumbaly, Pau Rodriguez, and David Vazquez. 3rd continual learning workshop challenge on egocentric category and instance level object understanding. *arXiv preprint arXiv:2212.06833*, 2022. URL https://sites.google.com/view/clvision2022/challenge.

Ameya Prabhu, Philip HS Torr, and Puneet K Dokania. Gdumb: A simple approach that questions our progress in continual learning. In *ECCV*, 2020.

Sylvestre-Alvise Rebuffi, Alexander Kolesnikov, Georg Sperl, and Christoph H Lampert. icarl: Incremental classifier and representation learning. In *CVPR*, 2017.

David Rolnick, Arun Ahuja, Jonathan Schwarz, Timothy Lillicrap, and Gregory Wayne. Experience replay for continual learning. *NeurIPS*, 2019.

Rik Sarkar. Low distortion delaunay embedding of trees in hyperbolic plane. In *International symposium on graph drawing*. Springer, 2011.

Qi She, Fan Feng, Xinyue Hao, Qihan Yang, Chuanlin Lan, Vincenzo Lomonaco, Xuesong Shi, Zhengwei Wang, Yao Guo, Yimin Zhang, et al. Openloris-object: A robotic vision dataset and benchmark for lifelong deep learning. In *ICRA*, 2020.

Guangyuan Shi, Jiaxin Chen, Wenlong Zhang, Li-Ming Zhan, and Xiao-Ming Wu. Overcoming catastrophic forgetting in incremental few-shot learning by finding flat minima. *NeurIPS*, 2021.

Haizhou Shi and Hao Wang. A unified approach to domain incremental learning with memory: Theory and algorithm. *NeurIPS*, 2024.

Ryohei Shimizu, Yusuke Mukuta, and Tatsuya Harada. Hyperbolic neural networks++. *arXiv preprint arXiv:2006.08210*, 2020.

Hanul Shin, Jung Kwon Lee, Jaehong Kim, and Jiwon Kim. Continual learning with deep generative replay. *NeurIPS*, 2017.

Arjun Singh, James Sha, Karthik S Narayan, Tudor Achim, and Pieter Abbeel. Bigbird: A large-scale 3d database of object instances. In *IEEE international conference on robotics and automation (ICRA)*, 2014.

Aditya Sinha, Siqi Zeng, Makoto Yamada, and Han Zhao. Learning structured representations with hyperbolic embeddings. *Advances in Neural Information Processing Systems*, 37:91220–91259, 2024.

Alexandru Tifrea, Gary Bécigneul, and Octavian-Eugen Ganea. Poincar\'e glove: Hyperbolic word embeddings. *arXiv preprint arXiv:1810.06546*, 2018.

Quyen Tran, Hoang Phan, Minh Le, Tuan Truong, Dinh Phung, Linh Ngo, Thien Nguyen, Nhat Ho, and Trung Le. Leveraging hierarchical taxonomies in prompt-based continual learning. *arXiv preprint arXiv:2410.04327*, 2024.

Abraham Albert Ungar. A gyrovector space approach to hyperbolic geometry. *Synthesis Lectures on Mathematics and Statistics*, 2008.

Gido M Van de Ven, Tinne Tuytelaars, and Andreas S Tolias. Three types of incremental learning. *Nature Machine Intelligence*, 2022.

Max van Spengler, Erwin Berkhout, and Pascal Mettes. Poincaré resnet. In *ICCV*, 2023.

Eli Verwimp, Kuo Yang, Sarah Parisot, Lanqing Hong, Steven McDonagh, Eduardo Pérez-Pellitero, Matthias De Lange, and Tinne Tuytelaars. Clad: A realistic continual learning benchmark for autonomous driving. *Neural Networks*, 2023.

Fu-Yun Wang, Da-Wei Zhou, Han-Jia Ye, and De-Chuan Zhan. Foster: Feature boosting and compression for class-incremental learning. In *ECCV*, 2022a.

Liyuan Wang, Kuo Yang, Chongxuan Li, Lanqing Hong, Zhenguo Li, and Jun Zhu. Ordisco: Effective and efficient usage of incremental unlabeled data for semi-supervised continual learning. In *CVPR*, 2021.

Liyuan Wang, Xingxing Zhang, Hang Su, and Jun Zhu. A comprehensive survey of continual learning: Theory, method and application. *TPAMI*, 2024.

Qiang Wang, Jiayi Liu, Zhong Ji, Yanwei Pang, and Zhongfei Zhang. Hierarchical correlations replay for continual learning. *Knowledge-Based Systems*, 2022b.

Yabin Wang, Zhiwu Huang, and Xiaopeng Hong. S-prompts learning with pre-trained transformers: An occam's razor for domain incremental learning. *NeurIPS*, 2022c.

Max Welling. Herding dynamical weights to learn. In *ICML*, 2009.

Yue Wu, Yinpeng Chen, Lijuan Wang, Yuancheng Ye, Zicheng Liu, Yandong Guo, and Yun Fu. Large scale incremental learning. In *CVPR*, 2019.

Cheng Yan, Feng Zhao, and Yudong Zhang. From concept to instance: Hierarchical reinforced knowledge graph reasoning. *IEEE Transactions on Emerging Topics in Computational Intelligence*, 2024.

Shipeng Yan, Jiangwei Xie, and Xuming He. Der: Dynamically expandable representation for class incremental learning. In *CVPR*, 2021.

Haiyan Yin, Ping Li, et al. Mitigating forgetting in online continual learning with neuron calibration. *NeurIPS*, 2021.

Yun Yue, Fangzhou Lin, Kazunori D Yamada, and Ziming Zhang. Hyperbolic contrastive learning. *arXiv preprint arXiv:2302.01409*, 2023.

Guanxiong Zeng, Yang Chen, Bo Cui, and Shan Yu. Continual learning of context-dependent processing in neural networks. *Nature Machine Intelligence*, 2019.

Friedemann Zenke, Ben Poole, and Surya Ganguli. Continual learning through synaptic intelligence. In *ICML*, 2017.

Bowen Zhao, Xi Xiao, Guojun Gan, Bin Zhang, and Shu-Tao Xia. Maintaining discrimination and fairness in class incremental learning. In *CVPR*, 2020.

Da-Wei Zhou, Fu-Yun Wang, Han-Jia Ye, Liang Ma, Shiliang Pu, and De-Chuan Zhan. Forward compatible few-shot class-incremental learning. In *CVPR*, 2022a.

Da-Wei Zhou, Qi-Wei Wang, Han-Jia Ye, and De-Chuan Zhan. A model or 603 exemplars: Towards memory-efficient class-incremental learning. *arXiv preprint arXiv:2205.13218*, 2022b.

Da-Wei Zhou, Qi-Wei Wang, Zhi-Hong Qi, Han-Jia Ye, De-Chuan Zhan, and Ziwei Liu. Deep class-incremental learning: A survey. *arXiv preprint arXiv:2302.03648*, 2023.

Chenchen Zhu, Fanyi Xiao, Andrés Alvarado, Yasmine Babaei, Jiabo Hu, Hichem El-Mohri, Sean Culatana, Roshan Sumbaly, and Zhicheng Yan. Egoobjects: A large-scale egocentric dataset for fine-grained object understanding. In *ICCV*, 2023.

Yudong Zhu, Di Zhou, Jinghui Xiao, Xin Jiang, Xiao Chen, and Qun Liu. Hypertext: Endowing fasttext with hyperbolic geometry. In *EMNLP*, 2020.

A Appendix

A.1 HyperCLIC algorithm pseudo code

Our method consists of two stages. The objective of the first stage (Algorithm 1) is to obtain a set of hyperbolic prototypes, which are later used in the second stage (Algorithm 2) for the classification loss:

Algorithm 1
3.1 Embedding class-instance hierarchies in hyperbolic space

Require: The joint class-instance hierarchy $\mathcal{T} = (V, E)$

We seek to obtain a set of prototypes $P = \{p_i\}_{i=1}^{|V|}$ corresponding to $V = \{v_i\}_{i=1}^{|V|}$ such that $d_{\mathbb{B}}(p_i, p_j) \propto d_{\mathcal{T}}(v_i, v_j)$
// Initialize prototypes with Poincaré loss:
for e in `#Poincaré_Epochs` **do**
    Minimize loss: $\mathcal{L}_{Poincaré} = \sum \log \frac{e^{-d_B(u,v)}}{\sum_{v' \in \mathcal{N}(u)} e^{-d_B(u,v')}}$
end for
// Enforce max-margin entailment regions:
for e' in `#Entailment_Epochs` **do**
    Minimize loss: $\mathcal{L}_{Entailment} = \sum E(u, v) + \max(0, \gamma - E(u', v'))$
end for
// Enforce separation between prototypes:
for e'' in `#Separation_Epochs` **do**
    Minimize loss: $\mathcal{L}_S(P) = \vec{1}^T(\bar{P}\bar{P}^T - I)\vec{1}$
end for
After obtaining the prototypes for all nodes in the tree $\mathcal{T}$, we only use the prototypes $P = \{P_y\}_{y=1}^{|V_I|}$ corresponding to the instance (leaf) nodes $V = \{v_y\}_{y=1}^{|V_I|}$ in the next stage.

Algorithm 2
3.2 Continual hyperbolic learning with hierarchical prototypes

Require: $P = \{P_y\}_{y=1}^{|V_I|}$

// The classification loss using prototypes from the previous stage:
$\mathcal{L}_{cls} = -\frac{1}{|\mathcal{D}^t|} \sum_{(x_i,y_i)\in\mathcal{D}^t} \sum_{i=1}^{|C|} y_i \cdot \log \left(\frac{e^{h(z_i^t, y_i)}}{\sum_{j=1}^{|C|} e^{h(z_i^t, y_j)}} \right)$
Keep a copy of the model parameters at time $t-1$ as θ^{t-1} to calculate the distillation loss:
$\mathcal{L}_{distil} = -\frac{1}{|\mathcal{D}^{b<t}|} \sum_{(x_i,y_i)\in\mathcal{D}^{b<t}} \sum_{i=1}^{|C^{b<t}|} p(y_i|z_i^{t-1}) \cdot \log p(y_i|z_i^t)$
Run network training by minimizing $\mathcal{L} = \mathcal{L}_{cls} + \mathcal{L}_{distil}$

A.2 Ablation: The effect of the number of fine-tuned layers

We observed that the results of our method and iCaRL differ based on the number of layers fine-tuned in the pretrained scenario. Figure 5 illustrates the impact on four hierarchical metrics as the number of fine-tuned layers varies for both methods. For iCaRL, increasing the number of fine-tuned layers results in worse performance, with lower instance-, class-, and superclass-level accuracies, and higher LCA distance. Conversely, for HyperCLIC, more fine-tuned layers lead to improved results. We hypothesize that this is because HyperCLIC enforces a hierarchical structure on the representations, and since the pretrained model was trained in Euclidean space, fine-tuning more layers allows HyperCLIC to leverage the model's capacity to learn hierarchically-aware representations from the first layer. Given these trends, we use the best scores for each method to compare HyperCLIC with the baseline in the pretrained scenario.

A.3 Statistical Significance

To evaluate the generality and stability of our method across different runs, we compare HyperCLIC with the best-performing baselines, iCaRL and DER, in both from-scratch and pretrained settings. Each experiment is conducted

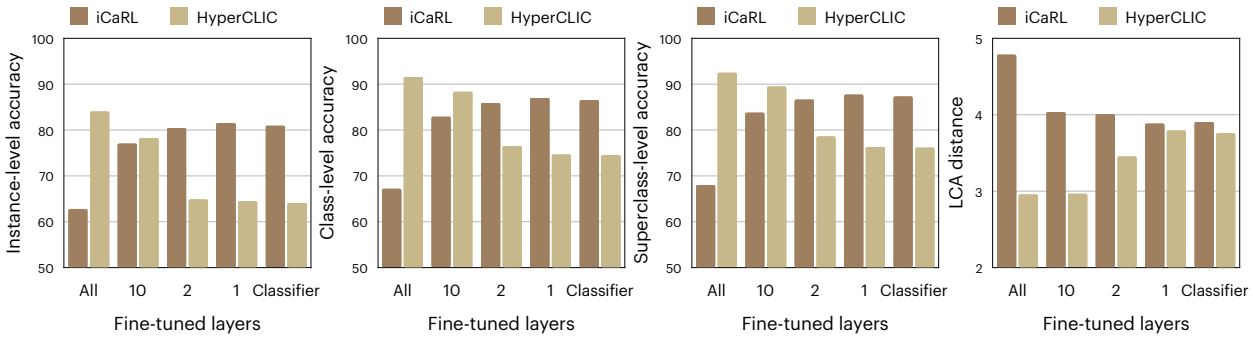


Figure 5: **Performance of HyperCLIC and iCaRL across four metrics** with varying numbers of fine-tuned layers. HyperCLIC excels when all layers are fine-tuned, while iCaRL performs better with more fixed layers. The Table 1 comparison in the pretrained scenario considers the optimal setup for each model.

Table 8: **Statistical Significance Testing (p-values) of HyperCLIC Compared with iCaRL and DER in From-Scratch and Pretrained Settings.** HyperCLIC demonstrates statistical significance compared to iCaRL and DER across all metrics, with a threshold of $p < 0.05$.

	From scratch				
	Instance	Class	Superclass	LCA	Forgetting
iCaRL	3.80e-7	1.46e-7	1.45e-7	1.19e-9	1.59e-4
DER	1.53e-6	5.79e-7	3.96e-7	2.71e-6	2.84e-10
	Pretrained				
	Instance	Class	Superclass	LCA	Forgetting
iCaRL	2.84e-2	1.61e-5	4.98e-6	1.76e-11	2.60e-2
DER	4.50e-2	9.29e-6	4.21e-6	2.07e-7	3.00e-3

using 5 different random seeds, and we report the average and standard deviation of the results in Table 9. Additionally, we perform statistical significance testing to compare HyperCLIC with the baselines. Table 8 presents the p-values for each metric. The results demonstrate that there are statistically significant differences between HyperCLIC and the two baselines across all metrics. Specifically, all p-values are below the commonly used threshold of $p < 0.05$, confirming that the observed performance improvements are statistically significant.

Extra Runs In continual learning, the order of class presentation can significantly affect the final results. To demonstrate the generality of our method, we run HyperCLIC and the best-performing baselines with 5 different random seeds in both from-scratch and pretrained settings on the EgoObjects benchmark, and report the average and standard deviations. Table 9 presents the results of this experiment. The findings suggest that HyperCLIC outperforms both DER and iCaRL in all metrics across both settings.

Table 9: **The average $\pm$ standard deviation of HyperCLIC , iCaRL, and DER, evaluated with 5 different random seeds in both from-scratch and pretrained settings on the EgoObjects benchmark.** HyperCLIC outperforms both strong baselines across all metrics.

	Pretrain	**Accuracy ↑**			**LCA ↓**	**Forgetting ↓**
		Instance	Class	Superclass		
iCaRL		21.49 ± 0.91	22.51 ± 0.87	23.62 ± 0.85	5.45 ± 0.01	8.72 ± 1.15
DER		18.69 ± 2.63	19.89 ± 2.58	20.56 ± 2.47	5.46 ± 0.10	33.90 ± 1.18
HyperCLIC		38.55 ± 2.37	42.74 ± 2.50	44.68 ± 2.63	4.91 ± 0.03	3.34 ± 1.39
iCaRL	✓	81.63 ± 0.20	87.03 ± 0.15	87.77 ± 0.16	3.91 ± 0.01	3.74 ± 0.30
DER	✓	80.73 ± 0.59	85.37 ± 0.83	86.13 ± 0.80	4.15 ± 0.16	9.98 ± 0.53
HyperCLIC	✓	83.14 ± 1.24	90.83 ± 0.91	91.75 ± 0.81	2.94 ± 0.03	5.61 ± 1.5